Sedimentology (2004) **51,** 455–477 doi: 10.1111/j.1365-3091.2004.00632.x

The cyclic hierarchy of the 'Purbeckian' Sierra del Pozo Section, Lower Cretaceous (Berriasian), southern Spain

EDWIN J. ANDERSON
Department of Geology, Temple University, Philadelphia, PA 19122, USA
(E-mail: andy@temple.edu)

ABSTRACT

The lowermost Cretaceous (Berriasian) Sierra del Pozo Formation is divisible into metre-scale cycles that are bundled in a four-tiered hierarchy of cycles and cyclic sequences. At the smallest scale, sixth-order cycles, thought to be the product of precessionally forced sea-level fluctuations (*c.* 20 ka), average less than a metre in thickness, shallow upward and are bounded by surfaces where deeper facies abruptly overlie shallower facies. Bundles of sixth-order cycles, called fifth-order sequences, are recognized by two types of asymmetric patterns in facies distribution. First, more pronounced facies changes occur at sixth-order cycle boundaries lower in a sequence, whereas smaller facies changes occur at cycle boundaries higher in a sequence. Secondly, subtidal marine limestones (i.e. biomicrites and biosparites) are the dominant facies lower in a cyclic sequence, whereas more restricted or shallower water facies (i.e. mud-cracked microbial laminites, dolomites, shale and clay) are more predominant higher in a cyclic sequence. The bundling of sixth-order cycles is explained as a product of periodic change (100 ka) in the eccentricity of the earth's orbit. The degree of orbital eccentricity modulates the magnitude of precessional sea-level fluctuations, which in turn determine the relative facies contrasts at sixth-order cycle boundaries. Larger scale fourth- and third-order sequences are defined by similar patterns in facies contrast at successive sequence boundaries and by a change in predominant facies type from bottom to top. These patterns are explained as the product of 400 ka and 2 Ma periodic variations in the eccentricity of the earth's orbit. In summary, the strength of the precessional signal varies in consort with periodic changes in orbital eccentricity at three time scales producing a stacked hierarchy of cycles and sequences of cycles. Change in obliquity of the earth's axis may modulate the effects of the precessional signal and thereby modify patterns of preserved cyclic structure. This interpretation of cyclicity in the Sierra del Pozo section is markedly different from that of Jiménez de Cisneros & Vera (1993), who attributed all rock cycles to a single process (obliquity) even though the cycles they described varied in thickness from less than 1 m to more than 4 m. The cycles they described are shown here to be either precessional cycles or composite sets of precessional cycles (100 ka sequences). In this new hierarchical interpretation, ninety-six 100 ka and twenty-four 400 ka sequences are recognized, extending the time of deposition of the Sierra del Pozo section to more than 9·6 Ma.

Keywords Berriasian, cyclostratigraphy, orbital forcing, 'Purbeckian', Spain.

INTRODUCTION

Jiménez de Cisneros & Vera (1993) described subtidal, intertidal and supratidal sedimentary facies in the 'Purbeckian' at the Sierra del Pozo section near Cazorla in southern Spain. This site is located in the Prebetic Zone where 'Purbeckian' facies were previously interpreted as peritidal limestones, dolomites and marls (García-Hernández *et al.*, 1979). Based on these facies analyses, Jiménez de Cisneros & Vera (1993) presented a new cyclostratigraphic analysis of the section and interpreted the cycles they described as having a periodicity in the 'Milankovitch band'. They assumed a time interval of 5·5 Ma, based on calpionellid and benthic foraminiferal biostratigraphy, for deposition of the stratigraphic section comprising 141 cycles, and calculated an average cycle duration of slightly more than 39 ka. They concluded that, relative to the Milankovitch frequency band, these cycles most closely matched obliquity cycles. Applying a Fischer plot analysis to these data, they also recognized 400 ka bundles of the small-scale cycles in the lower parts of the section.

The purpose of this paper is to re-evaluate the cyclic analysis of the Sierra del Pozo section of the 'Purbeckian' by the application of a hierarchical allocyclic model. This hierarchy is based on the 'Croll–Milankovitch' orbital forcing model described by Berger (1988) and Fischer & Bottjer (1991). Imbrie & Imbrie (1979) have comprehensively summarized the historical development of these ideas in their very readable book on the people involved in 'the search for a solution to the ice-age mystery'. Specifically, the entire Sierra del Pozo section was remeasured based on assumption of a four-tiered orbital-forcing model that predicts a stratigraphic record composed of elementary cycles plus a three-tiered hierarchy of cyclic bundles or sequences. The resulting new log is then compared with the stratigraphic log of Jiménez de Cisneros & Vera (1993, fig. 5, redrafted here as Fig. 1). Their stratigraphic facies analysis and cyclic log are of excellent quality and reproducible based on the new observations. Minor differences in measurement and only one significant difference in facies interpretation are discussed later.

The new hierarchical cyclic analysis presented below divides the 'Purbeckian' of the Sierra del Pozo section into twenty-four 400 ka sequences that are grouped into five 2 million year third-order sequences. These are shown on Fig. 1 superimposed on the log of Jiménez de Cisneros & Vera (1993). Each 400 ka (fourth-order) sequence is composed in turn of four 100 ka (fifth-order) sequences. Two consecutive fourth-order sequences are described and illustrated in two new logs and interpreted with the aid of detailed field photographs to illustrate fifth-order sequences and sixth-order precessional cycles typical of the overall section. The stratigraphic interval selected for detailed analysis includes cycles 53–64 of Jiménez de Cisneros & Vera (1993) (see black bar on Fig. 1, between 120 and 143 m on their log). This interval contains the first two fourth-order sequences in the third third-order sequence of the Berriasian. This new interpretation is then compared with the interpretation of Jiménez de Cisneros & Vera (1993).

GEOGRAPHICAL LOCATION

The Sierra del Pozo section is unique in that 'Purbeckian' facies (cyclic peritidal and marginal marine facies) are both unusually thick and nearly continuously exposed. The section occurs along the forest road (just south of the mountain pass, Puerto Llano) 12 km south (but 20 km along the gravel forest road) of Parador Nacional del Adelantado in the Parque Natural de Cazorla (Fig. 2). Specifically, the base of the section occurs where the Barranco del Escalon crosses the forest road 100 m north-west of the 24 km marker on the forest road. The section extends uphill along the road to a point 200 m west of the 23 km marker, 1·5 km south-west of Cabañas, the highest peak in the Sierra del Pozo (see the 1:50 000 Pozo Alcón topographic map, #21-38).

TIME-STRATIGRAPHIC POSITION

The section of the Sierra del Pozo Formation on the forest road is nearly three times as thick ($\approx$ 300 m) as the type section of the 'Purbeckian' in Dorset, UK. This marked difference in thickness occurs between the Spanish and Dorset sections even though in both areas the sections are thought to be approximately coincident with the Berriasian stage (Allen & Wimbledon, 1991; Clements, 1993; Jacquin *et al.*, 1998). Correlations of the 'Purbeckian' in Dorset (Allen & Wimbledon, 1991; Ogg *et al.*, 1994), the French Jura (Strasser & Hillgärtner, 1998) and southern Spain (Jiménez de Cisneros & Vera, 1993) with boundaries of the Berriasian stage are based on

calpionellid biozones (zones B, C, D1, D2 and D3), Tethyan and Boreal ammonite zones and magnetic chrons.

Ogg *et al.* (1991, 1994) showed the correlations between global magnetic chrons (specifically the base of chron 19 normal to the lower part of chron 14 reversed) and magnetic chrons that they had determined in the Berriasian to lower Valanginian sequence in Dorset. These correlations make available approximately 7 Ma in the Berriasian with an uncertainty in the dates of the lower and upper boundaries of 144·2 ± 2·6 Ma and 137 ± 2·2 Ma respectively (Gradstein *et al.*, 1995; Hardenbol *et al.*, 1998a) plus an additional million years in the lower Valanginian. Ogg *et al.* (1994) then correlated the chrons in Dorset to Boreal and Tethyan ammonite zones and the above-mentioned calpionellid zones (see also Jacquin *et al.*, 1998). These correlations imply that the thinner Dorset and Jura sections encompass as much time as the thicker 'Purbeckian' facies in the Sierra del Pozo section shown by Jiménez de Cisneros & Vera (1993, their fig. 4) to encompass calpionellid zones B, C and D1.

Given that facies in the Sierra del Pozo section (García-Hernández *et al.*, 1979; Jiménez de Cisneros & Vera, 1993; Vera & Jiménez de Cisneros, 1993) are similar to those in Dorset (Clements, 1993; Anderson, 2004) and the Jura (Strasser, 1994; Strasser & Hillgärtner, 1998), the Spanish section appears to be significantly more complete in terms of the number of cycles preserved and cycle thickness. Alternatively, deposition of the Sierra del Pozo section extended over a longer time interval than the sections in the Jura or Dorset, an interpretation in conflict with the correlation and time analysis presented by Jiménez de Cisneros & Vera (1993, p. 516).

SEQUENCE STRATIGRAPHY AND CYCLOSTRATIGRAPHY

Current methods of stratigraphic interpretation often work deductively from the models of sequence stratigraphy (Van Wagoner *et al.*, 1988; Vail *et al.*, 1991) and 'Croll–Milankovitch orbital forcing' or 'cyclostratigraphy' (Goodwin & Anderson, 1985, p. 515; Fischer & Bottjer, 1991; House, 1995; D'Argenio *et al.*, 1997). Strasser (1994) and Strasser & Hillgärtner (1998) used both these models in the interpretation of 'Purbeckian' facies at Mt Salève in the French Jura. To arrive at their interpretation, they first described the lithology (constructing a detailed stratigraphic log), interpreted the repetitive facies patterns and integrated these data with the biostratigraphic and chronostratigraphic framework of the Berriasian and Valanginian stages. They then evaluated their stratigraphic log in terms of the Croll–Milankovitch orbital-forcing model. The result is a log that depicts the section at Mt Salève as a three-tiered stacked hierarchy comprising elementary sequences (20 ka), small-scale sequences (100 ka bundles of elementary sequences) and medium-scale sequences (400 ka sets of small-scale sequences). They then integrated this orbitally forced cyclic hierarchy with 10 'third-order sequences' (Van Wagoner *et al.*, 1988), bounded by sequence boundaries (Be1 to Va3) as currently defined by Hardenbol *et al.* (1998a,b).

While three tiers of this hierarchy are attributed to orbital forcing, i.e. precession, short eccentricity and long eccentricity, the 10 'third-order sequences' are defined strictly in the sequence-stratigraphic terms of Vail *et al.* (1991) and Hardenbol *et al.* (1998a,b). Although Strasser (1994), Strasser & Hillgärtner (1998) and Strasser *et al.* (1999) then applied the terminology of sequence stratigraphy (e.g. transgressive surface, maximum flooding surface and sequence boundary) to each scale of the orbitally forced hierarchy, the relationship of the genetically determined cyclostratigraphic units to the standard internal structure of 'third-order sequences' is unclear.

The difficulty in merging the sequence-stratigraphic and cyclostratigraphic models lies in the issue of reconciling the defined internal structure of third-order sequences (see Van Wagoner *et al.*, 1988; Vail *et al.*, 1991; Kamola & Van Wagoner, 1995) with an orbitally forced cyclic hierarchy (see Gale *et al.*, 2002). In sequence stratigraphy, third-order sequences are divided into systems tracts (parasequence sets) that are in turn divided into parasequences, conformable sequences of beds bounded by marine flooding surfaces (Vail *et al.*, 1991). Van Wagoner *et al.* (1988) stated that these sequence-stratigraphic units are not by definition associated with specified thicknesses, time intervals of formation or particular regional or global causes.

While parasequences (the smallest scale units of sequence stratigraphy) are like elementary sequences (Strasser, 1994) or punctuated aggradational cycles (PACs; Goodwin & Anderson, 1985) in that the boundaries of each are marine flooding surfaces, parasequences are fundamentally different from elementary sequences and PACs in both their time implications and their hierarchical stacking patterns. First, Vail *et al.*

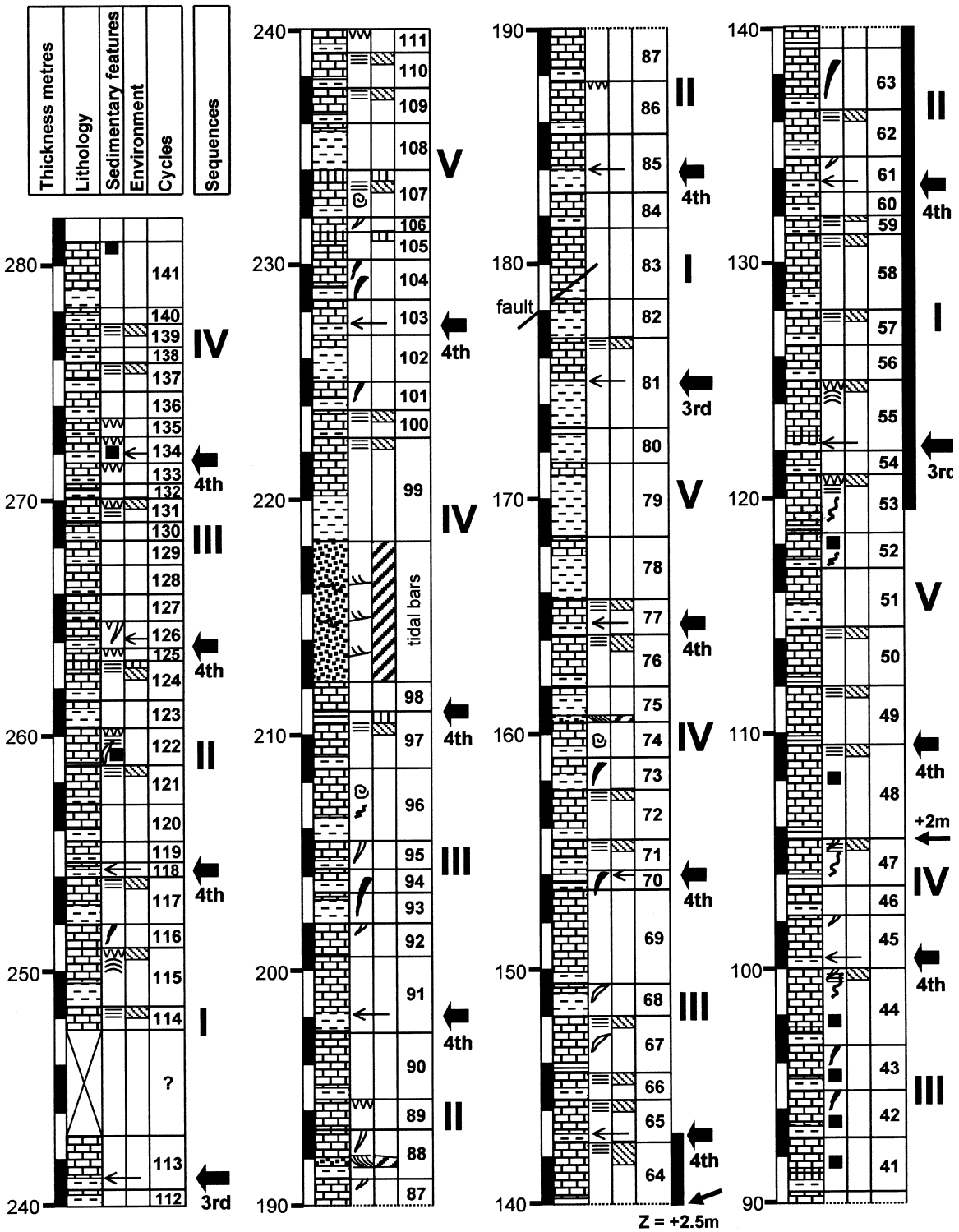

Fig. 1. Redrafted version of the stratigraphic log of Jiménez de Cisneros & Vera (1993, fig. 5). The location of interpreted third- and fourth-order sequences added at the right margin of the columns with fourth-order sequences numbered I to V. The position of two intervals of missing section noted at 106 and 140 m. Bar at right of column (120–143 m) indicates section described in detail.

(1991) acknowledged that 'periodic parasequences are believed to be caused by climatic fluctuations associated with Milankovitch scale orbital cycles (less than 500 ka)'. Therefore, this parasequence definition encompasses 20 ka, 100 ka and 400 ka cycles and cyclic sequences

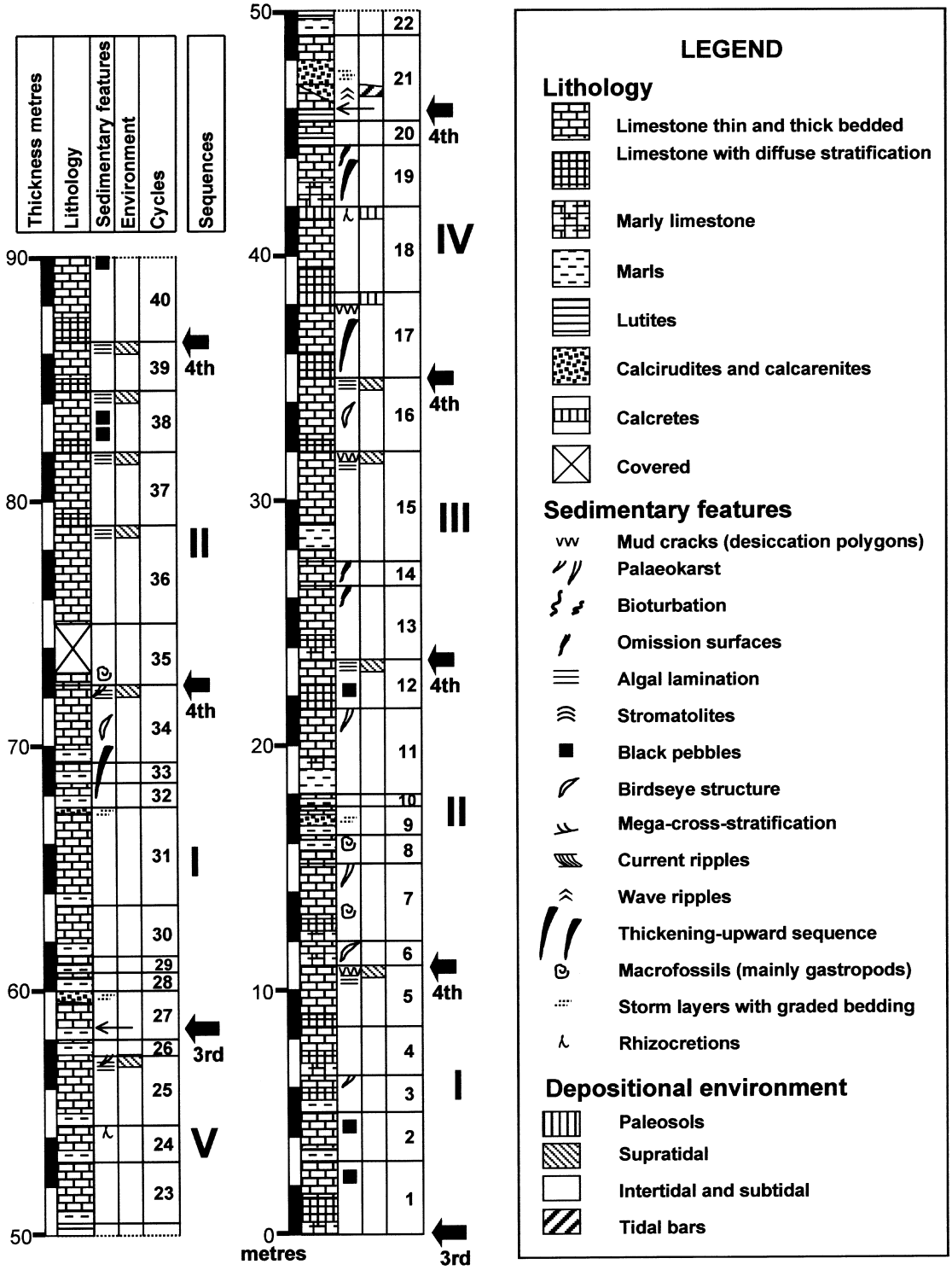

Fig. 1. (Continued).

(i.e. the sixth, fifth and fourth orders used in this paper). Secondly, while parasequences stack into aggradational, retrogradational and progradational parasequence sets (i.e. systems tracts), the internal structure of third-order sequences in sequence stratigraphy, elementary sequences and PACs stacks into a hierarchy of 100 ka, 400 ka and 2 Ma sequences. These differences suggest that the palaeogeographic and stratigraphic implications of these two methods may be in conflict. Einsele & Ricken (1991) briefly discussed the relationship of the orbitally forced cyclic

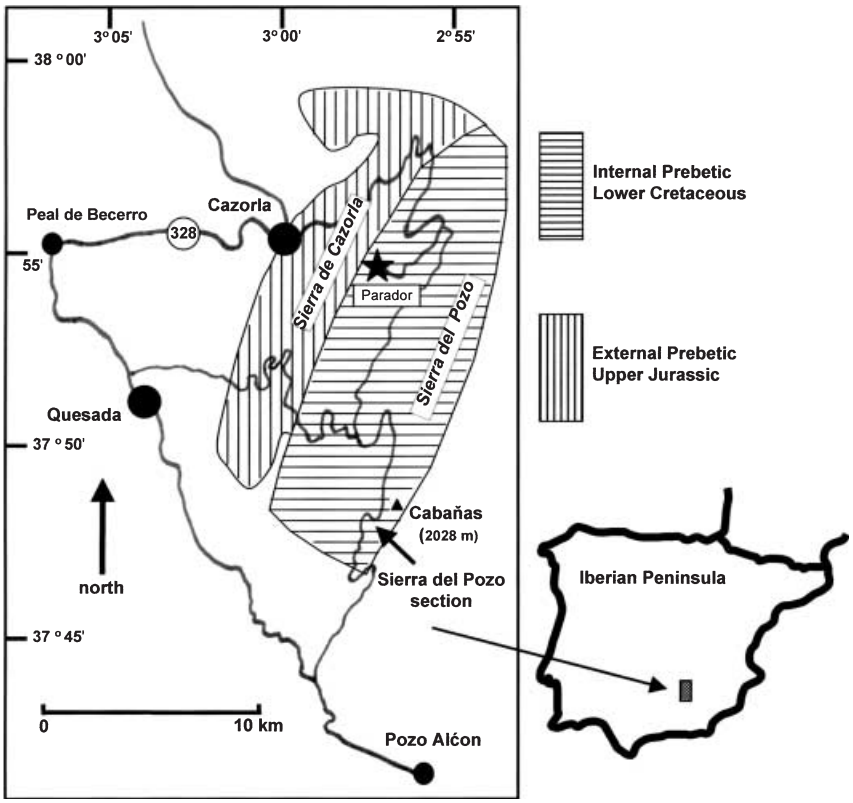

Fig. 2. Map showing the location of the Sierra del Pozo section on the forest road 12 km south of the Parador in the Parque Natural de Cazorla. Cazorla is located north-east of Granada in southern Spain, 170 km from Granada along the main highway that goes through Jaén, Bailén and Úbeda.

hierarchy to sequence stratigraphy and acknowledged some of the difficulties in integrating the orbital hierarchy and systems tracts. This same idea is expressed by Gale *et al.* (2002), who stated that the relationship between Milankovitch cycles and the third-order sequences of sequence stratigraphy remains enigmatic.

Vail *et al.* (1991) defined stratigraphic signatures that are associated with tectonic, eustatic, sedimentological or climatic processes. They grouped these process signatures into orders of duration from first order to sixth order (e.g. third order 0.5–3 Ma, fourth order 0.08–0.5 Ma, fifth order 0.03–0.08 Ma and sixth order 0.01 to 0.03 Ma). They then stated that parasequences or simple sequences (i.e. the building blocks of systems tracts and third-order sequences) form within the time durations of both fourth- and fifth-order cyclic processes (i.e. 0.03–0.5 Ma). In this formulation, parasequences do not comprise an orbitally forced hierarchy and are not placed within the time framework of sixth-order processes (i.e. the interval that includes the precessional signal).

Strasser & Hillgärtner's (1998) interpretation of the 'Purbeckian' of the Jura as a cyclic hierarchy based on orbital forcing (i.e. 100 ka and 400 ka bundles of elementary sequences) and (Anderson's (2004) interpretation of the correlative cyclic hierarchy in Dorset are fundamentally different from the defined internal structure of third-order sequences in the 'sequence-stratigraphic' model. While the boundaries of 20 ka, sixth-order cycles (elementary sequences or PACs) are marine flooding surfaces, these cycles are different from parasequences. In particular, parasequences are not constrained by time or thickness and thus, in practice, the 20 ka, 100 ka or even 400 ka sequences (of cyclostratigraphy) might all be identified as parasequences. Also, as explained above, parasequences are not conceived as part of an orbitally forced cyclic hierarchy but are a generalized type of shallowing-upward sequence representing a variable interval of deposition from 0.03 to 0.5 Ma (Vail *et al.*, 1991). Thus, an integrated set of parasequences assembled into three or four systems tracts (defining a third-order sequence) cannot be logically imposed on a multitiered orbitally forced cyclic hierarchy describing the same stratigraphic interval.

DEDUCTIVE METHODOLOGY

The following new cyclic interpretation of the Sierra del Pozo section adopts a strict deductive approach working from the predicted cyclic

hierarchy implied by the orbital-forcing model alone (Croll, 1875; Milankovitch, 1941; Berger, 1988). This deductive approach is consistent with the hypothetico-deductive interpretation of the scientific method (Popper, 1959), the views of Kuhn (1962) and those of Eldredge & Gould (1972) that science advances principally through the generation and testing of paradigms. That is, ideas precede detailed observations and, to a large degree, significant observations are only made under the influence of some previously formulated hypothesis (see Goodwin & Anderson, 1985).

The adoption of this method is reasonable, not because the hypothesis of orbital forcing has been proven to be a universal cause of sea-level fluctuation and in turn of stratigraphic cyclicity, but because a significant amount of published evidence implicates this process. For example, as mentioned above, in rocks of the same age and in similar facies, Strasser & Hillgärtner (1998) described a four-tiered hierarchy and attributed it to orbital forcing. Pittet *et al.* (2000) found a comparable four-tiered hierarchy and attributed it to the same forcing mechanism in the Oxfordian of Germany and southern Spain. They correlated this hierarchy of cycles between Spain and Germany and between deeper water and platform sections demonstrating the allogenic control on its formation. In slightly older Mesozoic rocks, Goldhammer *et al.* (1990) attributed a stacked hierarchy of cycles in the Latemar platform carbonates to composite sea-level oscillations, the 20 ka precessional and the 100 ka eccentricity signals (although their concept of cyclic orders is different). Likewise D'Argenio *et al.* (1997) applied the orbital-forcing model to later Cretaceous platform strata in Italy. Dozens of additional examples are found throughout the stratigraphic record (see symposium volumes, edited by Fischer & Bottjer, 1991; De Boer & Smith, 1994; House & Gale, 1995).

The deductive approach (i.e. assuming the implications of the orbital-forcing model) leads to a field-mapping method in the form of drawing detailed columnar logs of cycles and cycle sets (referred to here as sequences) and focuses attention on relative facies contrast at cycle boundaries. The results of applying this method are in turn a test of the assumed model. If the field observations are persistently in conflict with the model and deviations from the model predictions cannot be explained, the model must be rejected. If observations are consistent with predictions and anomalies have reasonable explanations, the model is supported (not proven but strengthened).

THE ASSUMED ORBITAL-FORCING MODEL

Beginning with the orbital-forcing variables, as summarized by Berger (1988), Fischer & Bottjer (1991), De Boer & Smith (1994) and House (1995), in this study it is assumed that the fundamental signal is the precessional signal (Anderson & Goodwin, 1990). The strength of this signal is directly related to the degree of eccentricity of the earth's orbit (Fig. 3). As eccentricity increases and summers occur near perihelion (in the precessional cycle), insolation at high latitudes reaches a maximum. If those summers are in a hemisphere with large areas of continent at high latitude, then high insolation values may trigger the melting of significant amounts of accumulated continental glacial ice. When summers occur near aphelion with high eccentricity, the resulting long series of cool summers may trigger renewed build up of high-latitude, continental glacial ice. While it has been suggested by many that the Mesozoic was a 'green house' world with no significant continental ice, recent work by Price (1999) provided new evidence of high-latitude continental glaciation at several times in the Mesozoic (including the Berriasian). He suggested that continental glacial ice might have been as much as 30% of the volume available in recent time. If this evidence is accepted, it removes the 'ice-free world' objection (see also Weissert & Lini, 1991). As summarized by Strasser *et al.* (1999), several mechanisms other than glacio-eustatic fluctuations are known to drive sea-level changes including thermal expansion and contraction of the ocean surface and seafloor spreading rates. However, it is difficult to explain cyclic bundling patterns with tectonic mechanisms or the magnitudes of sea-level rises with thermal expansion.

In concept, the orbital-forcing model leads to a pattern of sea-level fluctuation in response to varying insolation controlled by precessional cycles where the degree of rise and fall of sea level is proportional to the degree of eccentricity of the earth's orbit (Fig. 3). The ellipticity of the earth's orbit varies cyclically from near round to as much as 5% with a period of about 100 ka (see Berger, 1988). When eccentricity is high, there would be large changes in summer insolation (and potentially large ice volume and sea-level changes) between the perihelion and aphelion summer positions. When it is low, the amount of change in insolation through a precessional cycle would approach zero (stable sea levels). Secondarily, sets of 100 ka eccentricity cycles occur with

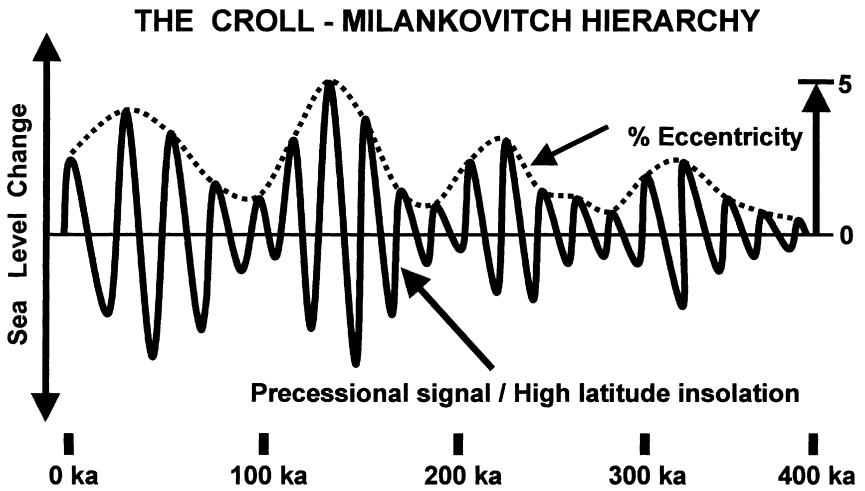

Fig. 3. Model summarizing the relationships among precession, eccentricity and sea level. When eccentricity (dotted line) is high, contrasts in summer insolation at high latitudes are at a maximum, forcing maximum precessional sea-level fluctuations (solid line). When eccentricity is minimal, precessional sea-level fluctuations are correspondingly small. This periodic change in degree of eccentricity bundles precessional sea-level fluctuations into sets of five. In a set of four eccentricity cycles, the second cycle is depicted as reaching an eccentricity maximum producing a 400 ka bundle (Goodwin & Anderson, 1997; Anderson, 2004).

enhanced peaks in eccentricity at 400 ka intervals (see Fig. 3; and Berger, 1988, p. 634).

The role of obliquity in the assumed orbital-forcing model is limited to modulating the magnitude of insolation changes through the precessional cycle. With increased tilt of the earth's axis, the planet experiences increased insolation at high latitudes. Thus, as tilt increases in the *c.* 40 ka obliquity cycle, coincident precessional sea-level rises should be magnified and, as tilt decreases, precessional sea-level rises should be muted. For example, if a maximum precessional sea-level rise were in phase with maximum tilt, the magnitude of this rise would be amplified but, 20 ka later, the next precessional rise would occur at minimum tilt and be muted. This could lead to a cyclic stratigraphic record in which the first precessional rise produced a marked facies change at the associated precessional (sixth-order) cycle boundary but where the next sixth-order boundary might be difficult to detect (see the 'Purbeckian' example discussed later).

STRATIGRAPHIC AND SEDIMENTOLOGICAL PROCESSES

Here, a distinction is drawn between processes that can be observed in modern sedimentary environments (called sedimentological processes) and processes that act over much longer time intervals, are allogenic vs. autogenic and are independent of common sedimentary processes (called stratigraphic processes). In the assumed model, all orbitally forced sea-level rises are primarily the product of the precessional signal. Therefore, all surfaces at allocycle boundaries, recognized by abrupt change from shallower to deeper facies, are the product of this mechanism (Anderson & Goodwin, 1990; Goodwin & Anderson, 1997). By extension, the surfaces that bound bundles of cycles (i.e. fifth- and fourth-order sequence boundaries) are also produced by this mechanism. Thus, the smallest scale cycles (sixth order), elementary sequences (Strasser, 1994) or PACs (Goodwin & Anderson, 1985), the fundamental units of cyclostratigraphy, are the product of a stratigraphic process (orbitally forced sea-level change). In this view, sedimentological processes are relevant only for interpreting the deposition of facies within cycles or sequences. In contrast, stratigraphic processes determine the boundaries of cycles and the structure of sequences of cycles.

To clarify this distinction, sedimentological processes act over short time intervals, that is minutes, hours, months or years. They are responsible for the deposition of grains, laminations and some beds and bed sets (Campbell, 1967) and can thus be studied in modern environments. Such processes are viewed as analogous to processes defined by Gould (1985) that control evolution at the 'first tier' (i.e. in the ecological moment). In contrast, stratigraphic processes operate at a much longer time scale and, to a large degree, act independently of the

sedimentological processes described above. Stratigraphic processes (and their products) are thought to be analogous to 'second' and 'third tier' processes defined by Gould (1985) as controls on larger scale patterns of evolution. They are typically eustatic and tectonic in origin and produce allogenic cycle boundaries, the bundling of cycles into sequences, unconformities and sedimentary basins.

The terms elementary sequence (Strasser, 1994) and PAC (Goodwin & Anderson, 1985, 1997) are applied exclusively to precessionally forced rock cycles. They are fundamentally the products of the stratigraphic processes that produce their boundaries (even though sedimentological processes deposit facies internal to them). Variation in the degree of eccentricity produces bundles of these rock cycles (fifth- and fourth-order sequences) by periodically forcing changes in the magnitude of the precessional signal (Fig. 3). This bundling by periodic changes in eccentricity is also a stratigraphic process. In a similar manner, Swift *et al.* (2003) drew distinctions between sedimentological and stratigraphic concepts.

CYCLE BOUNDARIES

It is proposed here that the boundaries of precessionally forced rock cycles are surfaces produced by rates of sea-level rise that exceed a critical value (Anderson, 2004). Above some critical rate of sea-level rise, carbonate production is disrupted, and terrigenous clastic sediments are trapped in fluvial plain environments producing a discontinuity in contemporaneous marginal marine and marine environments (Fig. 4). As sea level stabilizes, carbonate sediments are typically the first sediments to be deposited. Likewise, during sea-level falls, carbonate production may be disrupted, and a sea-level fall surface may be created. Landward erosion may then introduce terrigenous shale into marginal marine and shelf areas (as suggested by Strasser *et al.*, 1999) as lowstand facies.

Tipper (1997) discussed this issue of the formation of cycle boundaries at length and pointed out that 'there must be a lag between sea-level change and sedimentation' to produce cycle boundaries that define shoaling-upward cycles. He also stated that the parameters used in 'models' to switch off sedimentation and the lag phenomenon itself are totally different. He then developed colonization models for carbonate-producing organisms that predict rates of carbonate production in relation to rates of sea-level change and depth.

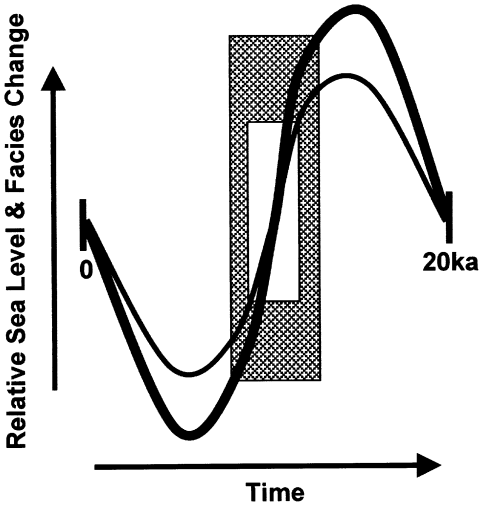

Fig. 4. Model illustrating the relationship between the magnitude of precessionally forced sea-level rise and degree of facies disjunction at sixth-order cycle boundaries. Sedimentation ceases at some critical rate of sea-level rise producing a cycle boundary surface. With higher magnitude rises, the critical rate is reached sooner and extends for a longer period of time, and a greater facies change (difference in depth) occurs across the boundary surface (outer box). With lower magnitude rises, the cycle boundary surface represents less time and a smaller facies change (difference in depth) produced by the interval of non-deposition (inner box). In like manner, a sea-level fall surface may be created if a critical relative rate of sea-level fall is reached. Highstand facies are deposited after sea-level rises and lowstand facies after sea-level falls. Alternatively, sea-level falls may expose highstand deposits to pedogenesis or erosion (Goodwin & Anderson, 1985, 1997; Anderson, 2004).

The simple model proposed here adopts Tipper's (1997) basic concepts concerning carbonate production, colonization and changing environmental stress with changing depth (combined eustasy and subsidence). At rates above some critical value of sea-level change, carbonate sedimentation effectively stops as colonization is disrupted by environmental stress related to depth change and the rate of that change. Higher amplitude sea-level rises produce discontinuities at cycle boundaries, representing longer time intervals and displaying larger facies contrasts across the boundary surface (Fig. 4).

Notice, as Tipper (1997) pointed out, that this concept of a mechanism for producing cycle boundaries is distinct from concepts using computer-generated lag time or lag depth (e.g. Read *et al.*, 1986) and is capable of explaining the genesis of cycle boundaries in totally subtidal

deposits. Strasser *et al.* (1999, p. 204) presented models for the development of cycle boundaries (i.e. elementary sequence boundaries) in both a shallow platform setting with emergence and a deeper water setting without emergence. In the emergent case, lag occurs during the sea-level rise producing a marked cycle boundary at an eroded and diagenetically altered surface. In the subtidal cycle, terrigenous clays deposited at sea-level lowstand mark the cycle boundary.

An estimated value for the critical rate of sea-level change can be derived by setting limits on the time interval of rise and the relative change in water depth associated with that rise. In the simple case of a symmetric sea-level curve produced by the precessional signal (period 20 ka), a third of the time interval of sea-level rise might be above the critical rate (e.g. 3–15 m of rise in 3000 years). This example produces a rate of 1–5 m per 1000 years. If the sea-level curve is asymmetric, with the rise occurring over shorter intervals, for the same amounts of rise, the rate could be two to four times higher (e.g. as much as 1 m per 100 years).

The critical value for rate of sea-level change may also be exceeded during (precessional) sea-level falls, producing sea-level fall surfaces within sixth-order cycles. Sea-level rise surfaces are more marked and better preserved stratigraphically because rates of relative sea-level rise are amplified by subsidence while rates of relative sea-level fall are diminished. Two lines of evidence support this model that relates cycle boundaries (sea-level rise surfaces) and sea-level fall surfaces to a critical rate of sea-level change. First, cycle boundary surfaces occur between subtidal cycles where there is no evidence of subaerial exposure and, secondly, sharp surfaces occur at the transition between highstand and lowstand facies produced by sea-level falls where the traditional lag concept would not apply. In this context, sea-level fall surfaces represent simple discontinuities within a single sixth-order (20 ka) cycle and are distinct from sequence boundaries recognized by patterns of onlap and offlap surfaces in 'sequence stratigraphic' models.

CYCLES VERSUS SEQUENCES

The term cycle is used to describe the smallest allocycle in the orbitally forced hierarchy, that is rock cycles produced by the precessional signal. In turn, the word sequence is used here to describe genetically determined sets or bundles of these cycles, in particular the 100 ka, 400 ka and 2 Ma year sets (see Anderson, 2004). The precessionally forced rock cycle is fundamental (Anderson & Goodwin, 1990) because all cycle and sequence boundaries are thought to be the product of precessionally forced sea-level rises. Periodic variation in the degree of eccentricity is only responsible for bundling precessional cycles (PACs of Goodwin & Anderson, 1985; elementary sequences of Strasser, 1994) into the larger scale hierarchy of sequences (Figs 3 and 5), not for independently producing its own rock cycles.

Finally, the word cycle is used to describe not a recurrent vertical sequence of facies, but a repeated pattern of events that produces a stratigraphic product. These events and products include: (1) sea-level rise disrupts deposition and produces a surface at which deeper facies overlie shallower facies; (2) return to sea-level stability (highstand) leads to renewed deposition, i.e. aggradation and filling of accommodation (i.e. shallowing); (3) sea-level fall results in additional facies shallowing (and possibly a sea-level fall surface overlain by lowstand facies); (4) the sequence of events is repeated. It is this pattern of events and products that is repetitive and periodic, i.e. cyclic (Goodwin & Anderson, 1985; Anderson & Goodwin, 1990; Anderson, 2004). The total thickness of a sequence of rock cycles as well as the thickness of many individual rock cycles is constrained by the accommodation produced by subsidence.

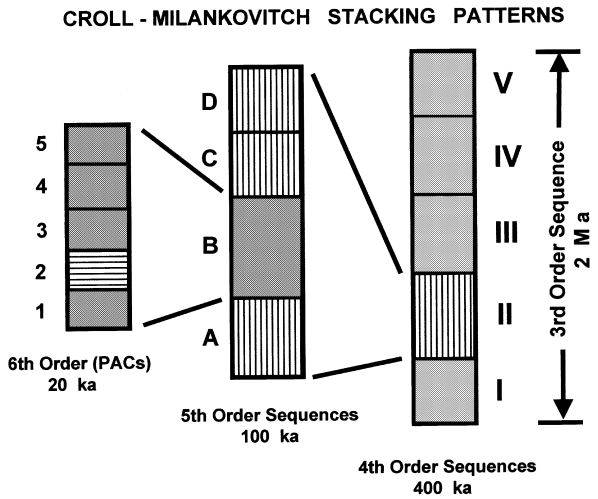

Fig. 5. Stacking patterns of cycles and sequences derived from assumption of the orbital-forcing model. With complete preservation, five sixth-order cycles (PACs) may occur in one fifth-order sequence and four fifth-order sequences in one fourth-order sequence. The largest facies contrasts or most open marine facies tend to occur in the second unit in each order (2, B or II) resulting in sequence asymmetry (Goodwin & Anderson, 1997; Anderson, 2004).

THE GENETIC HIERARCHY

The hierarchy of cycles applied in this study is genetic in the sense that each rank in the hierarchy is related to a specific stratigraphic process. In particular, as described above, fourth-, fifth- and sixth-order cycles (or sequences) are each related to a particular orbital-forcing process involving the interplay of precession and eccentricity. Third-order sequences, as defined in this paper, are bundles of five fourth-order (i.e. 400 ka) sequences that are recognized by patterns of facies asymmetry. They thus represent two million year bundles of fourth-order sequences.

However, use of the term 'third order' follows from the usage of 'sequence stratigraphy' where the fundamental unit is the 'third-order sequence' (a genetically related set of strata bounded by unconformities and their correlative conformities; Van Wagoner *et al.*, 1988). Although these 'third-order sequences' are not defined in terms of duration, in practice, third-order sequences tend to represent 1–2 Ma intervals of the stratigraphic record (see Vail *et al.*, 1991). It is thought here that the third-order sequence boundaries of the Berriasian stage (Hardenbol *et al.*, 1998a,b) bound sequences that are variable in duration because they are a mixture of 400 ka and 2 Ma sequence boundaries as defined in the orbitally forced hierarchical model of cyclostratigraphy (see Strasser *et al.*, 2000; Gale *et al.*, 2002). The fourth-, fifth- and sixth-order ranks used in this study as products of the orbital-forcing model are conceptually and genetically distinct from the hierarchy of stratal units used in the 'sequence stratigraphy' model discussed earlier (Van Wagoner *et al.*, 1988; Vail *et al.*, 1991; Kamola & Van Wagoner, 1995).

The genetically specific ranks used in this paper are also distinct from the 'orbitally related' hierarchy of orders used by Goldhammer *et al.* (1990) who applied time ranges in their definition of ranks (i.e. fifth order is 10–100 ka and fourth order is 100–1000 ka). In contrast, Brett *et al.* (1990; table 1) used a cyclic hierarchy that does attach specific periods to the 'Milankovitch band' ranks, but they also add a new rank (the subsequence with a period of 1·0–1·5 Ma). They also equate PACs of Goodwin & Anderson (1985, 1997) with the 100 ka rank. However, the PAC is defined as the product of the 20 ka precessional signal (Goodwin & Anderson, 1985; fig. 12; Goodwin & Anderson, 1997; Anderson, 2004).

If complete preservation of the orbitally forced hierarchy occurs, the predicted stacking pattern (where sixth-order cycles are the product of precession) consists of five sixth-order cycles in each fifth-order sequence. At the next level, four fifth-order sequences should occur in each fourth-order sequence and, at a larger scale, five fourth-order sequences are predicted in a third-order sequence (Fig. 5). The largest facies changes occur at the bases of sixth-order rock cycles and in the lower part of the second cycle or sequence in each of the larger scale bundles in the hierarchy. The rock record demonstrates that the basic cycle and the bundled sets of these cycles are asymmetric in facies distribution. It is most parsimonious to have the bundled sets reach a shallowest point (or a minimal facies contrast across cycle boundaries) towards the top or termination of larger scale sequences.

FACIES ANALYSIS

Jiménez de Cisneros & Vera (1993) provided a detailed facies analysis as a basis for defining shallowing-upward cycles in the Sierra del Pozo section. They provided a comprehensive set of lithological, biological and sedimentological features to interpret three facies (subtidal, intertidal and supratidal) and a fourth group of calcarenites and calcirudites interpreted as tidal channel bar deposits (Fig. 1). They described seven types of asymmetric cycles based on facies analysis and seven types of cycle capping surfaces representing different degrees of emersion (or lack thereof).

Subtidal facies

Jiménez de Cisneros & Vera (1993) stated that poorly stratified, nodular biomicrites and marly biomicrites (and locally fine calcarenites) occur at the bases of each of their defined cycles. These deposits occur as beds up to 1 m in thickness, contain lituolid foraminifera and dasycladacean algae and are interpreted as the products of a warm subtidal palaeoenvironment.

Intertidal facies

In the cyclically recurring facies pattern described by Jiménez de Cisneros & Vera (1993) finer grained greyish-white limestones, typically less than 0.5 m thick overlie the subtidal facies. These deposits are commonly unlaminated micrite and contain irregular (birdseyes) and laminoid fenestrae. Fossils are rare, but small miliolid foraminifera and large gastropods may occur associated

with the fenestral fabric. This facies may also contain black pebbles suggesting nearby emergent land areas (Vera & Jiménez de Cisneros, 1993) and burrows. This facies association is interpreted as intertidal.

Supratidal facies

The upper parts of many of the cycles defined by Jiménez de Cisneros & Vera (1993) consist of laminated limestones interpreted (by them) as planar to domal stromatolites. These deposits (that may be up to 1 m thick) commonly contain well-developed desiccation cracks and are interpreted as the product of microbial mats in a supratidal palaeoenvironment. The presence of black pebbles and thin intercalated layers of charophytes (freshwater) supports the interpretation of emergent conditions.

Cycle tops

Jiménez de Cisneros & Vera (1993) defined cycle tops on a variety of criteria indicating varying degrees of emergence. They used these criteria in consort with facies associations to define seven varieties of shallowing-upward cycles (also called sequences). Increasing degrees of emersion are indicated by sedimentary discontinuity, burrows or borings, coated hardgrounds, mud cracks, karst development, rhizoliths (calcretes) and calcareous breccias respectively. A geochemical and trace element analysis of two cycles (cycles 55 and 47) was carried out (by them) to develop an ideal sequence model for the peritidal carbonate palaeoenvironment.

For the present study, a new stratigraphic log of the entire Sierra del Pozo section was constructed on the outcrop. These field observations confirmed the facies analysis (summarized above) of Jiménez de Cisneros & Vera (1993) with only one significant exception. That is, apparently unfossiliferous clay/shale (marls), interpreted by Jiménez de Cisneros & Vera (1993) as subtidal facies and placed at the bases of cycles, are interpreted here as the most restricted facies in the overall sequence and placed at the top of cycles as lowstand deposits. Currently, three lines of evidence support this revised interpretation. The first is the persistent stratigraphic position of these thick clay/shale deposits (0.5–1 m) immediately above the shallowest carbonate facies in mapped cycles. They sometimes appear to be palaeosols containing black pebbles (Vera & Jiménez de Cisneros, 1993) or calcareous nodules (glaebules) and may overlie or penetrate into a palaeokarst. These deposits are then abruptly overlain by massive subtidal limestone facies (biomicrite and biosparite).

The second basis for this interpretation is related to a general hypothesis that relates the dynamic response of facies type to sea-level change. That is, fine-grained terrigenous sediment is thought to be introduced into basin-margin (and deeper water) palaeoenvironments following a sea-level fall and consequent landward erosion (see discussion below). This mechanism for introducing terrigenous clay/shale into carbonate platform and basinal facies has been suggested for similar facies in the 'Purbeckian' of the Jura (Strasser *et al.*, 1999) and for the Cenomanian of the Anglo-Paris Basin (Gale *et al.*, 2002).

The third line of evidence is comparison of these clay/shale deposits with similar deposits in the Purbeck sections of Dorset currently being studied by the author and Dennis Terry (a palaeosol specialist at Temple University). In Dorset, 35 palaeosol profiles have been recognized and described. Based on the presence of pedogenic slickensides, jarosite, root traces, aquic features, blocky peds and abundant plant remains, these palaeosols are classified as sulphahemists, sulphaquepts and sulphaquents. Each of these profiles is represented by a clay/shale deposit and is between 0.25 and 1 m thick. The profiles display strong development of horizonation with black and grey clay layers overlying relict-bedded shale. The clay layers contain well-developed root traces with pyritic and jarositic staining along with coalified and charcoal fragments, indicating that these profiles represent former acid sulphate soils. All these palaeosols occur at the top of previously identified sixth-, fifth- and fourth-order cycles or sequences, i.e. these palaeosols occur in the same cyclostratigraphic position as the clay/shale intervals in the Sierra del Pozo section.

FACIES RESPONSE TO SEA-LEVEL RISE AND FALL

As described by Jiménez de Cisneros & Vera (1993) for Spain, Clements (1993) for Dorset and Strasser (1994) for the Jura, 'Purbeckian' facies are predominantly marginal marine to brackish and freshwater carbonates, marls and shales. In this palaeoenvironmental setting, it is argued here that the first deposits that overlie a sea-level rise

surface are carbonates. It is thought that fine-grained terrigenous sediments were trapped landward as coastal plains aggraded in response to the associated rise in base level. Thus, when sedimentation commenced following a sea-level rise, only carbonate grains were available in the marginal marine palaeoenvironments. Conversely, following sea-level falls (falling base level), landward coastal plain erosion led to a return of terrigenous sedimentation in the now more restricted marginal marine palaeoenvironments.

The consequence of applying this model to the interpretation of cycles in stratigraphic sections of the 'Purbeckian' is that cycle boundaries (i.e. sea-level rise surfaces) are nearly always placed at surfaces where carbonate rocks abruptly overlie unfossiliferous clay/shale beds (see stratigraphic logs, Figs 6 and 9). As indicated above, this interpretation is supported in several cases by a progressive shallowing sequence of facies into the clay/shale units and, in Dorset, by the development of palaeosols on a similar clay/shale facies containing pedogenic slickensides, horizonation and in places iron-stained and jarositic root structures (see Anderson, 2004).

MEASUREMENT OF THE SIERRA DEL POZO SECTION

Applying the above-described hierarchical orbital-forcing model, a new columnar cyclic log of the Sierra del Pozo Formation was constructed. In preparation for this task, every cycle boundary recorded by Jiménez de Cisneros & Vera (1993) was located and marked. It was possible confidently to locate their cycle boundaries because the measurements on their log are excellent. To ensure the matching of the cycle boundaries on their column with the field exposure, 15 key stratigraphic markers shown on their columnar log (Fig. 1) were located. These markers included the brown quartz-rich pebble beds in their cycles 21, 75, 88 and between 98 and 99, beds with large gastropods in cycles 8, 74, 96 and 107 and the coarse calcirudite in cycle 27. In addition, the fault in cycle 83, the soil in 124, the covered intervals at 74 and 245 m and the cycles depicted in fig. 9A in their 1993 paper (note the middle cycle in their figure, marked with an arrow, is their cycle 47) served as marker horizons.

A new cyclic log of the entire section was then constructed at a scale of 1 m to the inch. The resulting columnar log reflects, not a single type of cycle throughout, but ubiquitously shows a stacked hierarchy of cycles that approximates the assumed orbital-forcing model being applied (and thus tested). The third-, fourth- and fifth-order tiers in the hierarchy match the stacking pattern model illustrated in Fig. 5. However, fifth-order sequences contain a range from two to six elementary or sixth-order cycles, suggesting incompleteness in the cyclic record at this scale. The measurements on the new log are remarkably consistent with those of Jiménez de Cisneros & Vera (1993, their fig. 5 redrawn as Fig. 1 here). The location of third- and fourth-order sequences, the largest scale sequences described in this paper, is shown at the right hand side of Fig. 1.

Differences between their log, which is 280 m thick, and the new log (that records 296 m of section) are nearly entirely accounted for at four specific stratigraphic intervals. Their columnar log (Fig. 1) omits 2 m (a cycle) between their cycles 47 and 48; it also omits 2·5 m between their 63/64 and 64/65 cycle boundaries (this interval is marked Z on Figs 1 and 9). An additional 4·5 m is estimated (in the new measurements) for a poorly exposed interval at the position of their cycle 20. Finally, the 296 m of the new log includes a 4 m thick covered interval at the top of the section. These additions together sum to just over 13 m and, when subtracted from the total thickness measured, result in a cumulative difference of less than 3 m in the overall thickness (280 vs. 283 m) of the stratigraphic section.

HIERARCHIC CYCLIC ANALYSIS

A well-exposed, 25 m thick interval of the Sierra del Pozo section is presented here to illustrate a representative example of the complete cyclic hierarchy discovered by re-evaluation of the section using the hierarchical orbital-forcing model (Figs 5–10). This stratigraphic interval coincides with Jiménez de Cisneros & Vera (1993) cycles 53–65 (black bar in Fig. 1). A summary of the positions of the cycles on their published log (cycles 53–65) is shown on the left side of Figs 6 and 9.

A graphic lithofacies log with weathering profile is shown in the middle of Figs 6 and 9. In these selected samples from the new log of the entire section, the weathering profile emphasizes the contrast between carbonate-dominated beds and intervening marl or shale-rich intervals. These detailed logs also depict mud-cracked polygons in flat-laminated carbonate stromatolites, karst features, bedding thickness and style,

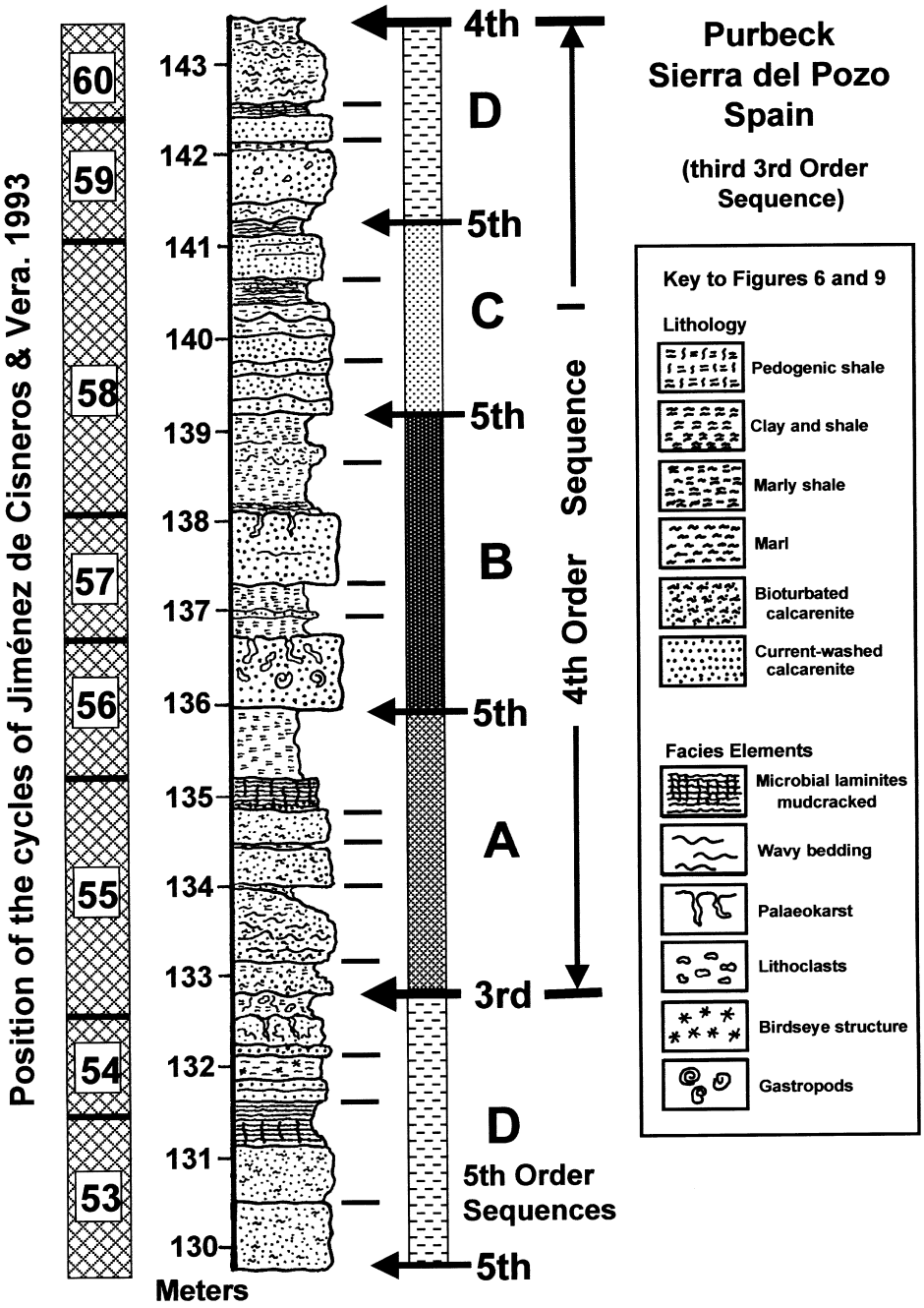

Fig. 6. Stratigraphic log of fourth-order Sequence I. Columnar lithological description and interpreted cyclic hierarchy on right and cyclic interpretation of Jiménez de Cisneros & Vera (1993, adapted from their fig. 5) for the same interval on left. In the cyclic hierarchy depicted on the right, tick marks designate sixth-order cycle boundaries. Fifth-order bundles are labelled A, B, C and D; the surfaces at third-, fourth- and fifth-order boundaries are designated with labelled arrows. See text for discussion of lithological features that define various types of cycles and their boundaries. Lithological log shows bedding and lamination thickness and weathering profile. Marls and shale (double dashes) are depicted as re-entrants and limestone units project outwards. Grain-size, bioturbation and mud cracks are indicated in the limestones.

apparent grain size and occasional fossils. The log is drawn to look as much like the rock exposure as possible (compare these new logs with field photographs in Figs 7, 8 and 10). The interval marked with a Z (Figs 1 and 9) was omitted from the Jiménez de Cisneros & Vera (1993) log, resulting in their cycle 64 being 2·5 m thinner than the interval shown here.

The right sides of Figs 6 and 9 depict the detailed hierarchical cyclic interpretation of the studied

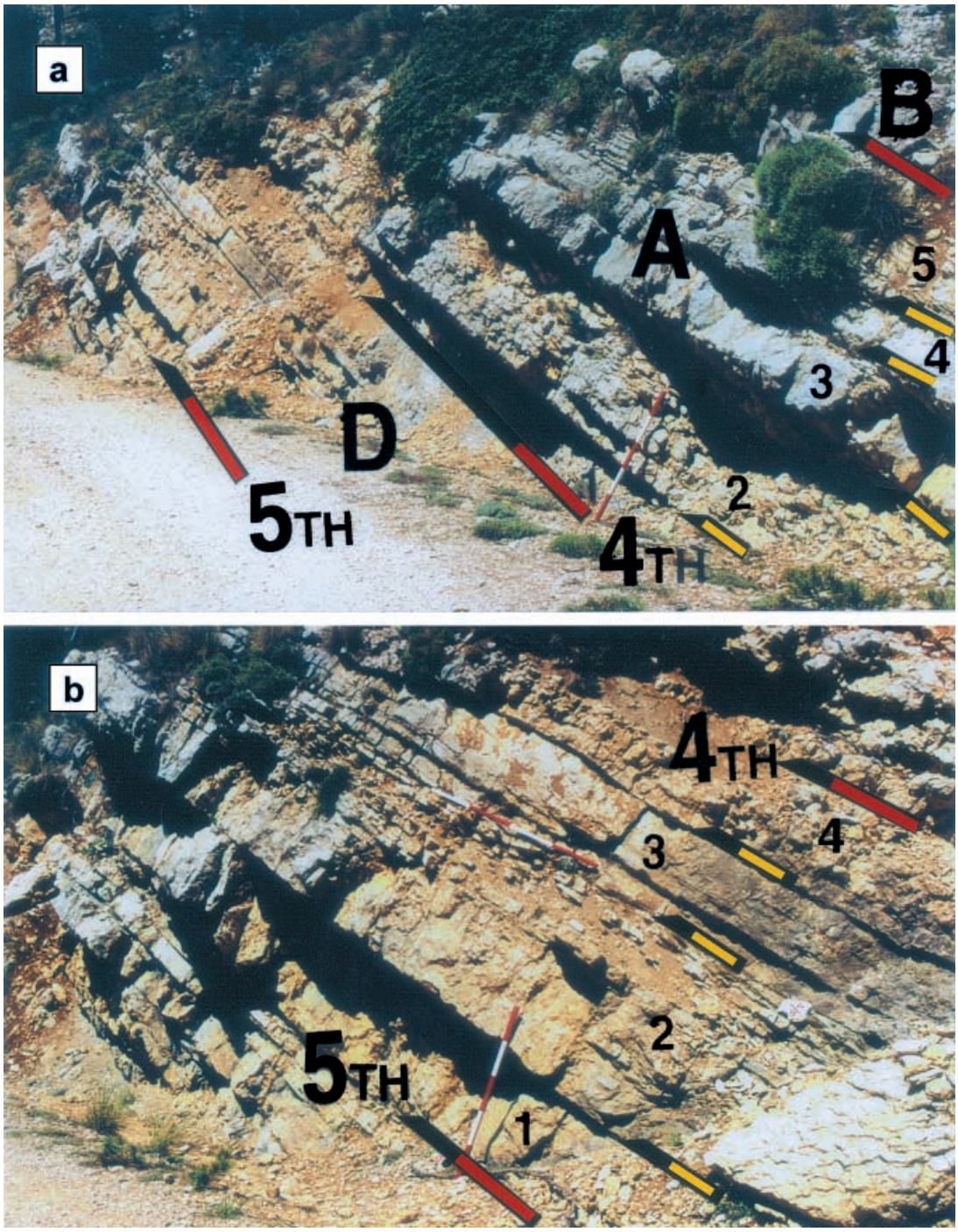

Fig. 7. The third/fourth-order boundary at 132·8 m on Fig. 6, the base of Sequence I. (a) The first fifth-order sequence above the fourth-order boundary. This sequence (A) begins at the surface at the base of the metre scale. The top of sequence A occurs above a 0.8 m thick marl/shale bed (covered) that overlies 0.3 m of polygonally cracked flat stromatolites seen in the top right hand corner of the picture. Sequence A is divisible into five PACs at surfaces marked with arrows. (b) The fourth-order boundary occurs above a palaeosol (line near top right corner). The base of the underlying fifth-order sequence (D) is at the surface at the base of the metre scale. It contains four PACs (boundary surfaces at arrows). See tick marks in the interval between 129·8 and 132·8 m on the column in Fig. 6.

interval. Two fourth-order sequences (Sequences I and II) are shown, with the upper and lower boundaries of each fourth-order sequence designated by an arrow labelled 4th. Each fourth-order sequence is divided into four fifth-order sequences labelled A, B, C and D. Subdivision of fifth-order

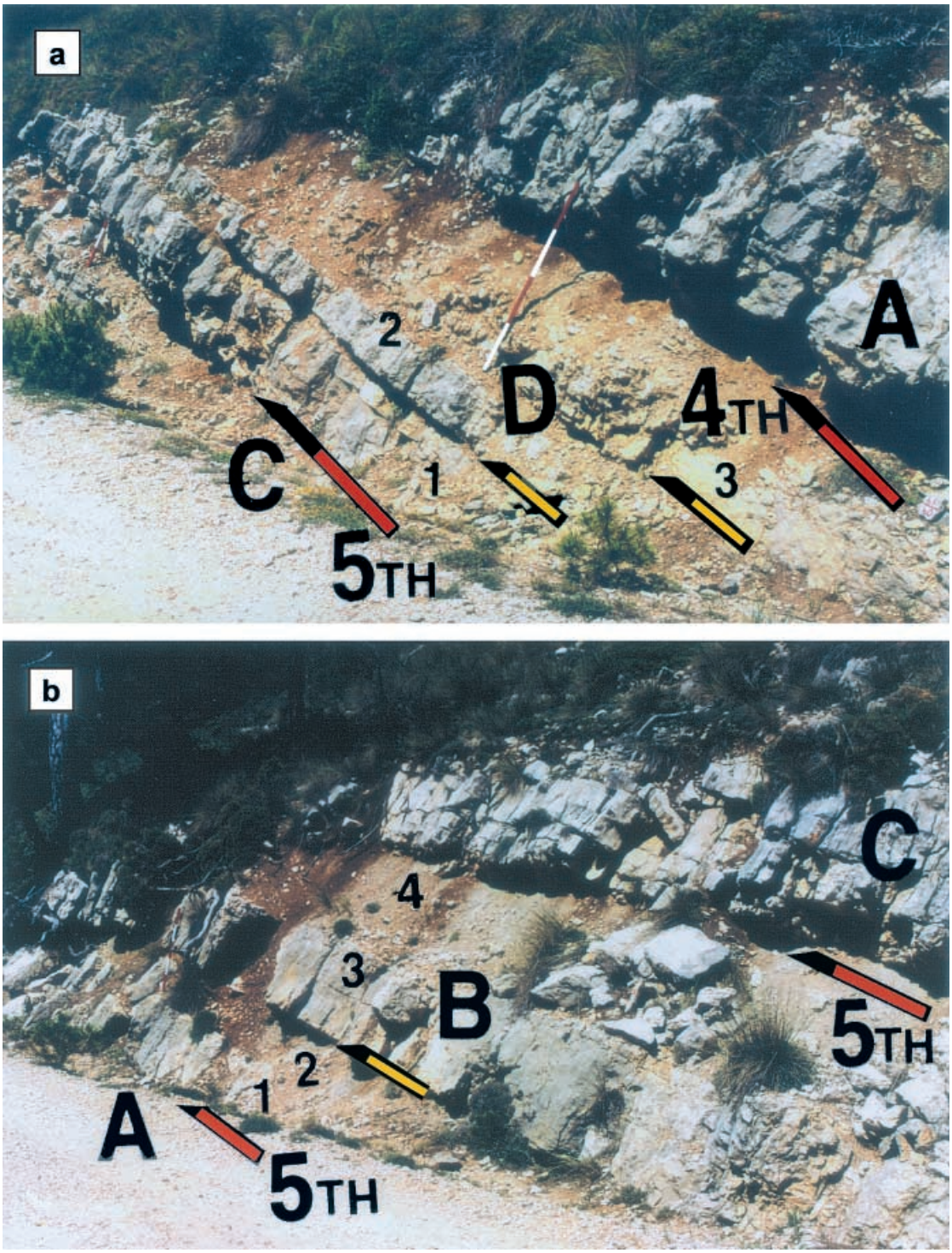

Fig. 8. Field photographs of fifth-order sequences B, C and D in Sequence I. (a) The base of fifth-order sequence D is at the base of the massive limestone bed marked C/D (red arrow). The top of sequence D, the fourth-order boundary, labelled D/A, is at the surface below the massive limestone bed at the top of the photo (at the 3-foot mark on the scale). Sequence D is divided into three PACs marked with yellow arrows (see Fig. 6). Most of the first PAC in sequence A just above the fourth-order boundary at 143·4 m (see Fig. 9) is seen at the top of the photo. (b) The base of fifth-order sequence B is at the base of the massive limestone bed (lower red arrow) seen below the metre scale labelled A/B (136 m on Fig. 6). The sequence top is the surface below the thick-bedded limestone unit (upper red arrow) in the top third of the photo labelled B/C (139·2 m on Fig. 6). This sequence is divided into four PACs (see Fig. 6), only two of which (1 and 3) have prominent facies change at their bases (see obliquity discussion in text).

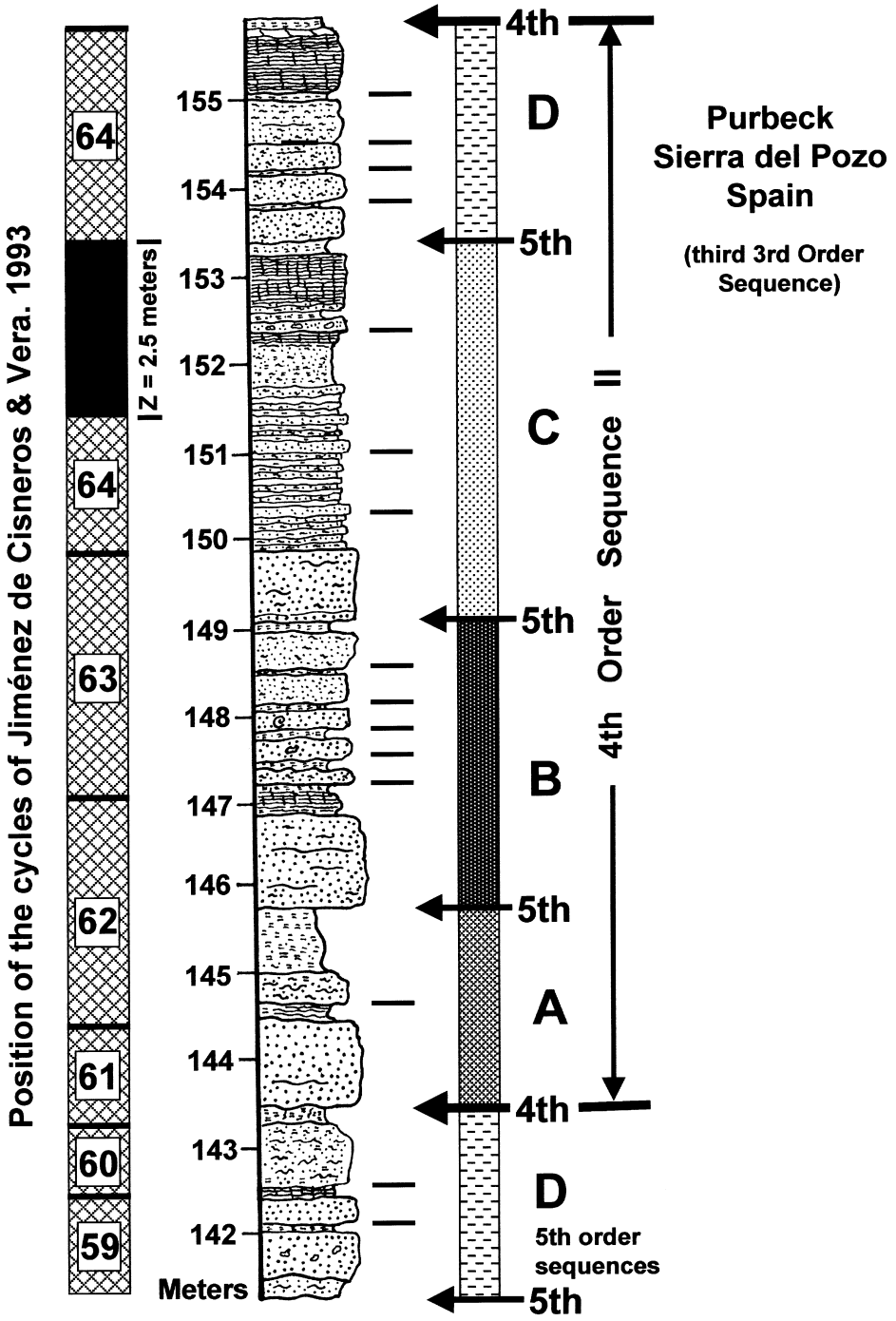

Fig. 9. Stratigraphic log of fourth-order Sequence II. A continuation of the cyclic stratigraphic log shown in Fig. 6. The location of the cycle boundaries of Jiménez de Cisneros & Vera (1993) is shown on the left. The interval labelled Z was omitted from their log (see text). A graphical representation of lithologies is shown on the right with an interpretation of the hierarchic cyclic structure applying the same conventions as in Figs 6 and 5. See text for discussion of the relationship between lithologies and cycle boundaries. Lithological features as in Fig. 6.

sequences into sixth-order cycles (PACs) is denoted by small tick marks at the cycle boundaries. In both the illustrated fourth-order sequences, the deepest facies or largest facies contrasts appear in the fifth-order B sequences. The shallowest or most restricted facies such as microbial laminites (often mud-cracked) are more dominant in sequences A, C and D.

A marked asymmetry characterizes the facies distribution in fifth-order sequences. In every

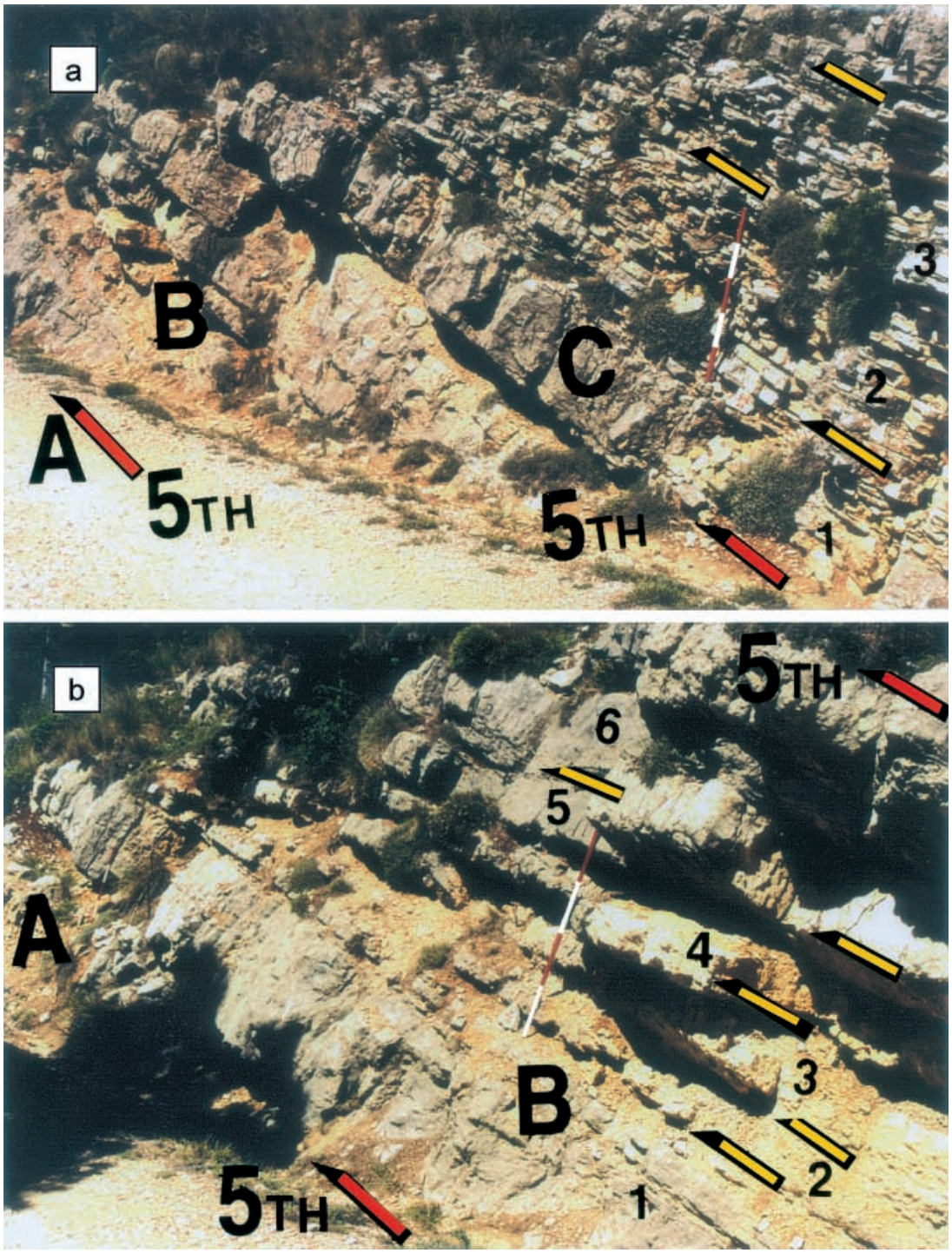

Fig. 10. Field photographs of fifth-order sequences B and C in Sequence II. (a) The base of fifth-order sequence C is at the base of the massive limestone bed just below the metre scale marked B/C. The top of the section seen in the photo is in the marly limestone at 152 m on Fig. 9. Thicker limestone beds (yellow arrows) at 150·3 and 151 m on Fig. 9 mark the bases of PACs in the thin-bedded unit in the top half of the section in the photo. Jiménez de Cisneros & Vera (1993, fig. 5, redrafted here as Fig. 1) showed their cycle 64 to be ≈3·2 m thick. The lower metre is thin-bedded limestone (the interval behind the metre scale in the photo), while the upper 2·2 m is thick-bedded limestone with algal lamination in the upper half (see Fig. 1). The interval between 151 and 153·5 m (Fig. 9) appears to be missing from their log. (b) The base of fifth-order sequence B is at the surface below the massive bed marked A/B behind the metre scale on the far left (lower red arrow); the top of sequence B is at the top right corner of the photo (see sequence B in Fig. 9). Sequence B is divided into six PACs; cycle boundaries are at surfaces at the base of limestone beds designated by arrows; thin marls occur at the top of each cycle.

case, in the illustrated stratigraphic interval, fifth-order sequences begin with massive generally coarser grained limestone beds (see Figs 6 and 9), whereas the tops of these sequences are represented by unfossiliferous clay/shale or marl deposits that frequently overlie mud-cracked stromatolites or palaeokarstic surfaces (see earlier discussion of the dynamic response of facies to sea-level rise and fall).

The two illustrated fourth-order sequences (Figs 6 and 9) are the first and second fourth-order sequences, respectively, in a larger scale third-order sequence. Subsequent fourth- and fifth-order sequences in this third order (not shown) contain less normal marine/more restricted facies (less massive carbonate and more marl–shale facies) and in general display smaller facies contrasts at cycle boundaries. This facies asymmetry (in part) defines this third third-order sequence and is characteristic of facies asymmetry in each of the third-order sequences in the Sierra del Pozo section (see Fig. 1).

COMPARATIVE CYCLIC ANALYSIS

Jiménez de Cisneros & Vera (1993) described 141 cycles in the 280 m of the Sierra del Pozo section. Their cycle boundaries (e.g. see left side of Figs 6 and 9) are defined at surfaces where subtidal facies abruptly overly tidal-flat facies, at surfaces where there is evidence of exposure (i.e. karst or palaeosols) or at marked facies discontinuities or bored hardgrounds. They consistently interpreted shales and marls as deeper water facies and placed all occurrences of this facies at the bases of cycles (e.g. see their cycles 56, 57 and 58 in Fig. 6). Cycle thicknesses on their complete log (varying between 1 and 4 m and averaging 1·98 m) are precise and reproducible. They concluded that the average duration of their cycles was $\approx$39 ka (based on dividing the 5·5 Ma estimated duration of the Berriasian by their total number of cycles). This time interval suggested that either precession or obliquity-forced sea-level change was the most probable explanation of the origin of these cycles and that the best fit for the average duration of these cycles was the obliquity-forcing mechanism.

Re-evaluation of the cyclicity in the Sierra del Pozo section, applying a 'Croll–Milankovitch-based' hierarchical genetic model (Anderson & Goodwin, 1990; Goodwin & Anderson, 1997; Anderson, 2004), suggests that the thicker cycles described by Jiménez de Cisneros & Vera (1993) are composite cycles. These composite cycles frequently approximate the 100 ka sequences interpreted in this paper (e.g. see their cycles 55, 58, 63 and 64 in Figs 6 and 9). Conversely, the thinner metre-scale cycles that they recognized often correspond to sixth-order cycles shown in Figs 6 and 9 (e.g. 60 and 61, with reversal of the shale facies interpretation) interpreted here as the product of the precessional signal and bundled in a four-tiered hierarchy.

The new cyclic hierarchy described for the Sierra del Pozo section conforms well to the multitiered cyclic structure described by Strasser & Hillgärtner (1998) in rocks of the same age (and similar facies) in the French Jura. The hierarchical stacking pattern observed in both the Jura and Spain, set within the established time constraints of the Berriasian and lowest Valanginian (Hardenbol *et al.*, 1998a,b), supports a 'Croll–Milankovitch' orbital-forcing mechanism.

THE FIRST ILLUSTRATED FOURTH-ORDER SEQUENCE

The first of two fourth-order sequences selected for illustration occurs between 132·8 and 143·5 m in the Sierra del Pozo section (Fig. 6, Sequence I). This sequence begins at the surface (Fig. 7a and b) where a sequence of thick limestone/thin shale couplets abruptly overlies a palaeosol (loose marl with lime mud nodules). The palaeosol in turn sits on a karst surface at 132·5 m, Jiménez de Cisneros & Vera (1993) boundary 54/55. The three PACs (sixth-order cycles or elementary sequences of Strasser, 1994) underlying the third/fourth-order boundary display criteria for subaerial exposure (the palaeosol and karst, birdseye micrite at 132 m and polygonally cracked stromatolites respectively; see Figs 6 and 7b). The overlying fifth-order sequence (sequence A) begins with four PACs dominated by subtidal facies. Only the last sixth-order cycle in sequence A is predominantly supratidal (a 4 cm thick calcarenite bed, the initial bed in this cycle, is overlain by polygonally cracked flat stromatolites followed by a lowstand shale; Figs 6 and 7a). Sequence A appears to be complete in that it comprises five precessional cycles.

Only four sixth-order cycles are seen in sequence B, where the first and third cycle boundaries are enhanced (they are surfaces of large facies change; Figs 6 and 8b) while the second and fourth cycle boundaries are muted.

This might be the result of the obliquity signal being temporarily in phase with the precessional signal (as discussed earlier). Sequences C and D comprise only three sixth-order cycles each, the top two in each case ending in laminated and/or mud-cracked facies (Figs 6 and 8a). These fifth-order sequences have smaller facies contrasts at cycle boundaries than sequences A and B below, reflecting the asymmetry of the fourth-order sequence.

THE SECOND ILLUSTRATED FOURTH-ORDER SEQUENCE

The second illustrated fourth-order sequence (Fig. 9, Sequence II) begins at 143·4 m and ends at 155·9 m. Each of the four fifth-order sequences begins at a surface below a massive limestone bed and ends in a lowstand shale (discussed below). Thick polygonally cracked microbial laminites also occur high in the upper two fifth-order sequences (Fig. 9, ≈153 and 155·5 m). Sequence A contains only two precessional cycles, while sequences B, C and D are nearly complete, each comprising four to six metre-scale cycles or PACs. This fourth-order sequence contains, on average, the most open marine, most carbonate-rich facies in the larger scale sequence in which it occurs, defining it as the second fourth order in a third-order bundle (Figs 1 and 5). Note that this relatively more open marine facies near the base of the third third-order sequence in the Sierra del Pozo section is tentatively correlated with relatively more open marine facies in the third third-order sequences in both Dorset (the Cinder member fourth-order sequence; Anderson, 2004) and the French Jura (Pierre Châtel Formation; Strasser & Hillgärtner, 1998).

The base of sequence A is the massive limestone behind the top of the four-foot scale in Fig. 8a. The bases of sequences B and C are also massive limestone beds, i.e. the thick bed ending a foot below the four-foot scale (Fig. 10b) and the massive bed just below the metre scale (Fig. 10a). The sequence of beds in sequence B between 147·2 and 149 m is interpreted here as a composite set of precessional cycles (Fig. 10b). These units are part of a 'thickening-upward sequence' of beds in Jiménez de Cisneros & Vera (1993) cycle 63 (compare Figs 1 and 9). The bases of PACs within sequence C are discriminated by slightly thicker calcarenite beds (at 150·2, 151 and 152·3 m; Fig. 9) in what is overall a thin-bedded unit.

SHALE VS. CARBONATE DEPOSITION

There is a fundamental difference in the interpretation of shales, marls or clay beds in the lithological logs developed for this paper (Figs 6 and 9) from that of Jiménez de Cisneros & Vera (1993). They consistently interpreted these facies (fine terrigenous sediments) as deeper water deposits and placed them at the bases of cycles (e.g. see shales at the bases of their cycles 55, 56, 57 and 58; Fig. 6). It is agreed here that, when fine terrigenous sediments occur as fossiliferous marly limestones, they are deeper facies and should be placed at the bases of cycles (e.g. the type G cycles listed by Jiménez de Cisneros & Vera, 1993, p. 523). However, frequently shales occur as they do between 135 and 136 m or 145 and 146 m (see Figs 6 and 9) where they do not have obvious macrofossils, where there is evidence of exposure or palaeosols in the upper part and where they are abruptly overlain by massive subtidal limestones. In these cases, they are interpreted as lowstand deposits in the upper half of sixth-order cycles.

In contrast, it is proposed that non-argillaceous, massive, fossiliferous limestone beds were deposited at sea-level highstands that followed periods of non-deposition during precessional sea-level rises. Examples of this type of limestone bed include the two beds between 130 and 131 m (Figs 6 and 7b, behind the metre scale) and the two beds with bases at 133·2 and 134 m (Figs 6 and 7a, 50 cm above the metre scale). Other examples include the two beds with bases at 136 and 137·3 m (Figs 6 and 8b) and the bases of similar massive limestone beds seen at 143·4, 145·8 and 149·1 m (Figs 9, 8a and 10). These beds are the basal units in the first and/or second PACs in fifth-order sequences.

It is thought that the lithostratigraphic responses described above are the result of trapping of terrigenous fine-grained sediments in coastal plain palaeoenvironments following sea-level (stream base-level) rises leading to clean carbonate deposition in marginal marine and shelf areas. Consequent sea-level falls in turn lead to non-deposition (or erosion) on the coastal plain with bypassing of fine-grained terrigenous sediments to what would then be more restricted marginal marine and marine environments. In this model, high-amplitude rises and falls may occur in the same cycle, resulting in marked facies changes across both sea-level rise and sea-level fall surfaces (see PACs 1 and 3 in sequence B, Figs 6 and 8b).

CONCLUSIONS

Interpretation of the cyclic structure of 'Purbeckian' facies in the Sierra del Pozo Formation is strongly influenced by models adopted by the observer. Strict assumption of the 'Croll–Milankovitch' orbital-forcing model leads to recognition of a stacked hierarchy of rock cycles where each tier of the hierarchy can be related to a stratigraphic process. The fundamental, sixth-order, cycle (a PAC) is a product of the 20 ka precessional signal. This basic unit is bundled into sets (fifth-order sequences) by periodic changes in eccentricity over 100 ka. These 100 ka sequences are bundled again by longer term periodic change in degree of eccentricity into 400 ka sets (fourth-order sequences).

All cycle boundary surfaces are a product of precessionally induced sea-level rise. The magnitude of precessionally forced sea-level rise is a direct function of the degree of eccentricity of the earth's orbit. Surfaces that mark cycle boundaries are produced when a critical rate of sea-level rise is exceeded. The degree of facies change across one of these surfaces is determined by the magnitude of sea-level rise, which determines the rate of rise and in turn the duration of the disconformity at the cycle boundary. Such surfaces are the product of a stratigraphic process and are distinct from ordinary bedding surfaces and laminations that can be seen to form in modern sedimentary environments. Periodic change in the degree of eccentricity at two or more scales determines the magnitude of sea-level rises and falls and thus the degree of facies contrasts at successive cycle boundaries. Patterns in the degree of facies change in a succession of cycle boundaries are the primary evidence for interpreting the cyclic hierarchy in the Sierra del Pozo section.

The Sierra del Pozo section comprises 96 fifth-order (100 ka) sequences bundled into 24 fourth-order (400 ka) sequences. Every fifth-order sequence can be subdivided into two to six sixth-order (20 ka) rock cycles or PACs. This hierarchic cyclic structure is distinct from the cyclic analysis of these rocks presented by Jiménez de Cisneros & Vera (1993) but similar to that developed by Strasser & Hillgärtner (1998) for the 'Purbeckian' section at Mt Salève in the French Jura and by Anderson (2004) for correlative facies in Dorset, UK. The new cyclic hierarchy interpreted for Purbeck facies in the Sierra del Pozo section implies that the stratigraphic accumulation of these rocks took 9·6 Ma. This interval is consistent with the time interval available in the Berriasian and lowest Valangian stages as documented by Hardenbol *et al.* (1998a) and Jacquin *et al.* (1998).

ACKNOWLEDGEMENTS

Professor Juan Antonio Vera provided helpful advice as well as maps and photographs of the Sierra del Pozo section. The author also thanks Juan Antonio Vera and André Strasser for their detailed and constructive reviews of the manuscript. The project was supported by a National Science Foundation grant EAR-9902680 and by a 1998 Research Incentive Fund grant from Temple University.

REFERENCES

Allen, P. and **Wimbledon, W.A.** (1991) Correlation of NW European Purbeck-Wealden (nonmarine Lower Cretaceous) as seen from the English type-areas. *Cretaceous Res.*, **12,** 511–526.

Anderson, E.J. (2004) Facies patterns that define orbitally forced third, fourth, and fifth order sequences of sixth order cycles and their relationship to ostracod faunicycles: the 'Purbeckian' (Berriasian) of Dorset, England. In: *Cyclostratigraphy–an Essay of Approaches and Case Histories* (Eds B. D'Argenio, A.G. Fischer, I. Premoli Silva, H. Weissert and V. Ferreri), *SEPM Spec. Publ.*, **81,** 243–258.

Anderson, E.J. and **Goodwin, P.W.** (1990) The significance of meter-scale allocycles in the quest for a fundamental stratigraphic unit. *J. Geol. Soc. London*, **147,** 507–518.

Berger, A. (1988) Milankovitch theory and climate. *Rev. Geophys.*, **26,** 624–657.

Brett, C.E., Goodman, W.M. and **LoDuca, S.T.** (1990) Sequences, cycles and basin dynamics in the Silurian of the Appalachian Foreland Basin. *Sed. Geol.*, **69,** 191–244.

Campbell, C.V. (1967) Lamina, laminaset, bed and bedset. *Sedimentology*, **8,** 7–26.

Clements, R.G. (1993) Type section of the Purbeck Limestone Group, Durlston Bay, Swanage, Dorset. *Proc. Dorset Nat. Hist. Archaeol. Soc.*, **114,** 181–206.

Croll, J. (1875) *Climate and Time in their Geological Relations; a Theory of Secular Changes of the Earth's Climate.* Daldy, Ibister, London, 577 pp.

D'Argenio, B., Amodio, S., Ferreri, V. and **Pelosi, N.** (1997) Hierarchy of high-frequency orbital cycles in Cretaceous carbonate platform strata. *Sed. Geol.*, **113,** 169–193.

De Boer, P.L. and **Smith, D.G.** (1994) Orbital forcing and cyclic sequences. In: *Orbital Forcing and Cyclic Sequences* (Eds P.L. de Boer and D.G. Smith), *Int. Assoc. Sedimentol. Spec. Publ.*, **19,** 1–14.

Einsele, G. and **Ricken, W.** (1991) Introductory remarks. In: *Cycles and Events in Stratigraphy, Part II, Larger Cycles and Sequences* (Eds G. Einsele, W. Ricken and A. Seilacher), pp. 611–616. Springer-Verlag, Berlin.

Eldredge, N. and **Gould, S.J.** (1972) Punctuated equilibria: an alternative to phyletic gradualism. In: *Models in*

Paleobiology (Ed. T.J.M. Schopf), pp. 82–115. Freeman, San Francisco.

Fischer, A.G. and **Bottjer, D.J.** (1991) Orbital forcing and sedimentary sequences. *J. Sed. Petrol.*, **61,** 1063–1069.

Gale, A.S., Hardenbol, J., Hathway, B., Kennedy, W.J., Young, J.R. and **Phansalkar, V.** (2002) Global correlation of Cenomanian (Upper Cretaceous) sequences: evidence for Milankovitch control on sea level. *Geology*, **30,** 291–294.

García-Hernández, M., Rivas, P. and **Vera, J.A.** (1979) Distribución de las calizas de llanuras de mareas en el Jurásico del Subbético y Prebético. *Cuad. Geol. Univ. Granada*, **10,** 557–569.

Goldhammer, R.K., Dunn, P.A. and **Hardie, L.A.** (1990) Depositional cycles, composite sea-level changes, cycle stacking patterns and the hierarchy of stratigraphic forcing: examples from Alpine Triassic platform carbonates. *Geol. Soc. Am. Bull.*, **102,** 535–562.

Goodwin, P.W. and **Anderson, E.J.** (1985) Punctuated aggradational cycles: a general model of stratigraphic accumulation. *J. Geol.*, **71,** 515–534.

Goodwin, P.W. and **Anderson, E.J.** (1997) Stratigraphic incompleteness: Milankovitch in the Manlius at the margin. In: *Field Trip Guide* (Eds T.W. Rayne, D.G. Bailey and B.J. Tewksbury), *NY State Geol. Assoc. 69th Annu. Meeting*, pp. 237–249.

Gould, S.J. (1985) The paradox of the first tier: an agenda for paleobiology. *Paleobiology*, **11,** 2–12.

Gradstein, F.M., Agterberg, F.P., Ogg, J.G., Hardenbol, J., van Veen, P., Thierry, J. and **Huang, Z.** (1995) A Triassic, Jurassic and Cretaceous time scale. In: *Geochronology, Time Scales and Global Stratigraphic Correlation* (Eds W.A. Berggren, D.V. Kent, M.P. Aubry and J. Hardenbol), *SEPM Spec. Publ.*, **54,** 95–126.

Hardenbol, J., Thierry, J., Farley, M.B., Jacquin, T., De Graciansky, P.-C. and **Vail, P.R.** (1998a) Cretaceous sequence chronostratigraphy. In: *Mesozoic and Cenozoic Sequence Stratigraphy of European Basins* (Eds P.-C. De Graciansky, J. Hardenbol, T. Jacquin and P.R. Vail), *SEPM Spec. Publ.*, **60** (chart).

Hardenbol, J., Thierry, J., Farley, M.B., Jacquin, T., De Graciansky, P.-C. and **Vail, P.R.** (1998b) Mesozoic and Cenozoic sequence chronostratigraphic framework of European basins. In: *Mesozoic and Cenozoic Sequence Stratigraphy of European Basins* (Eds P.-C. De Graciansky, J. Hardenbol, T. Jacquin and P.R. Vail), *SEPM Spec. Publ.*, **60,** 3–13.

House, M.R. (1995) Orbital forcing timescales: an introduction. In: *Orbital Forcing Timescales and Cyclostratigraphy* (Eds M.R. House and A.S. Gale), *Geol. Soc. London Spec. Publ.*, **85,** 1–18.

House, M.R. and **Gale, A.S.** (eds) (1995) *Orbital Forcing Timescales and Cyclostratigraphy. Geol. Soc. London Spec. Publ.*, **85.**

Imbrie, J. and **Imbrie, K.P.** (1979) *Ice Ages.* Enslow Publishers, Hillside, NJ, 224 pp.

Jacquin, T., Rusciadelli, G., De Graciansky, P.-C. and **Magniez-Jannin, F.** (1998) The North Atlantic cycle: an overview of 2nd-order transgressive/regressive facies cycles in the Lower Cretaceous of Western Europe. In: *Mesozoic and Cenozoic Sequence Stratigraphy of European Basins* (Eds P.-C. De Graciansky, J. Hardenbol, T. Jacquin and P.R. Vail), *SEPM Spec. Publ.*, **60,** 397–409.

Jiménez de Cisneros, C. and **Vera, J.A.** (1993) Milankovitch cyclicity in Purbeck peritidal limestones of the Prebetic (Berriasian, southern Spain). *Sedimentology*, **40,** 513–537.

Kamola, D.K. and **Van Wagoner, J.C.** (1995) Stratigraphy and facies architecture of parasequences with examples from the Spring Canyon Member, Black Hawk Formation, Utah. In: *Sequence Stratigraphy of Foreland Basin Deposits* (Eds J.C. Van Wagoner and G.T. Bertram), *AAPG Mem.*, **64,** 27–54.

Kuhn, T.S. (1962) *The Structure of Scientific Revolutions*. The University of Chicago Press, Chicago, IL, 172 pp. (2nd edn, 1970, 210 pp.).

Milankovitch, M. (1941) *Kanon der Erdbestrahlung und seine Anwendung auf das Eiszeitenproblem.* Royal Serbian Academy, 132, Section of Mathematical and Natural Sciences, Belgrade, 633 pp. [Canon of Insolation and the Ice-Age Problem. English translation by Israel Program for Scientific Translations, Jerusalem, 1969].

Ogg, J.G., Hasenyager, R.W., Wimbledon, W.A., Channell, J.E.T. and **Bralower, T.J.** (1991) Magnetostratigraphy of the Jurassic–Cretaceous boundary interval – Tethyan and English faunal realms. *Cretaceous Res.*, **12,** 455–482.

Ogg, J.G., Hasenyager, R.W., II and **Wimbledon, W.A.** (1994) Jurassic–Cretaceous boundary: Portland–Purbeck magnetostratigraphy and possible correlation to the Tethyan faunal realm. *Geobios*, **17,** 519–527.

Pittet, B., Strasser, A. and **Mattioli, E.** (2000) Depositional sequences in deep-shelf environments: a response to sea-level changes and shallow-platform carbonate productivity (Oxfordian, Germany and Spain). *J. Sed. Res.*, **70,** 392–407.

Popper, K. (1959) *The Logic of Scientific Discovery*. Basic Books, New York, 479 pp.

Price, G.D. (1999) The evidence and implications of polar ice during the Mesozoic. *Earth-Sci. Rev.*, **48,** 183–210.

Read, J.F., Grotzinger, J.P., Bova, J.A. and **Koerschner, W.F.** (1986) Models for generation of carbonate cycles. *Geology*, **14,** 107–110.

Strasser, A. (1994) Milankovitch cyclicity and high-resolution sequence stratigraphy in lagoonal-peritidal carbonates (Upper Tithonian-Berriasian, French Jura Mountains). In: *Orbital Forcing and Cyclic Sequences* (Eds P.L. de Boer and D.G. Smith), *Int. Assoc. Sedimentol. Spec. Publ.*, **19,** 285–301.

Strasser, A. and **Hillgärtner, H.** (1998) High-frequency sea-level fluctuations recorded on a shallow carbonate platform (Berriasian and Lower Valanginian of Mount Salève, French Jura). *Eclogae Geol. Helv.*, **92,** 375–390.

Strasser, A., Pittet, B., Hillgärtner, H. and **Pasquier, J.-B.** (1999) Depositional sequences in shallow carbonate-dominated sedimentary systems: concepts for a high-resolution analysis. *Sed. Geol.*. **128,** 201–221.

Strasser, A., Hillgärtner, H., Hug, W. and **Pittet, B.** (2000) Third-order depositional sequences reflecting Milankovitch cyclicity. *Terra Nova*, **12,** 303–311.

Swift, D.J., Parsons, B.S., Foyle, A. and **Oertel, G.F.** (2003) Between beds and sequences: stratigraphic organization at intermediate scales in the Quaternary of the Virginia coast, USA. *Sedimentology*, **50,** 81–111.

Tipper, J.C. (1997) Modeling carbonate platform sedimentation – lag comes naturally. *Geology*, **25,** 495–498.

Vail, P.R., Audemard, F., Bowman, S.A., Eisner, P.N. and **Perez-Cruz, C.** (1991) The stratigraphic signatures of tectonics, eustasy and sedimentology – an overview. In: *Cycles and Events in Stratigraphy* (Eds G. Einsele, W. Ricken and A. Seilacher), pp. 617–659. Springer-Verlag, Berlin.

Van Wagoner, J.C., Posamentier, H.W., Mitchum, R.M., Vail, P.R., Sarg, J.F., Loutit, T.S. and **Hardenbol, J.** (1988) An overview of the fundamentals of sequence stratigraphy and

key definitions. In: *Sea-Level Changes an Integrated Approach* (Eds C.K. Wilgus, B.S. Hastings, C.G.StC. Kendall, H.W. Posamentier, C.A. Ross and J.C. Van Wagoner), *SEPM Spec. Publ.*, **42,** 39–45.

Vera, J.A. and **Jiménez de Cisneros, C.** (1993) Palaeogeographic significance of black pebbles (Lower Cretaceous, Prebetic, southern Spain). *Palaeogeogr. Palaeoclimatol. Palaeoecol.*, **102,** 89–102.

Weissert, H. and **Lini, A.** (1991) Ice age interludes during the time of Cretaceous greenhouse climate? In: *Controversies in Modern Geology* (Eds D.W. Müller, J.A. McKenzie and H. Weissert), pp. 173–191. Academic Press, London.

Manuscript received 5 November 2002;
revision accepted 20 October 2003.